

Michał Piątkowski  [orcid.org/0000-0002-4803-7561](https://orcid.org/0000-0002-4803-7561)

[michal.piatkowski@tu.koszalin.pl](mailto:michal.piatkowski@tu.koszalin.pl)

Environmental and Geodetic Sciences, Faculty of Civil Engineering, Koszalin University of Technology

## THE INFLUENCE OF THE GEOMETRY OF IMPERFECT TRUSSES ON THE LOADING OF TRANSVERSAL ROOF BRACINGS

### WPLYW GEOMETRII KRATOWNICY Z IMPERFEKCJAMI NA OBCIĄŻENIE POPZECZNEGO TĘŻNIKA DACHOWEGO

#### Abstract

Geometrical imperfections of compressed chords in truss girders generate loads on the transverse roof bracings which are connected to the truss girders. The real distribution of this load is contrary to the model presented in the EN 1993-1-1 standard. The influence of the shape of the truss girder with geometrical imperfections on the load of transverse roof bracing has been numerically analysed in this article. The most commonly used shapes of truss girders as well as selected geometrical parameters have been considered. The obtained research results were used to determine the load acting on roof purlins and bracing rods in a typical hall structure.

**Keywords:** geometry of truss, bracing, geometrical imperfections

#### Streszczenie

Imperfekcje geometryczne pasów ściskanych w dźwigarach kratowych wywołują obciążenie połączonych z nimi poprzecznych tężników połaciowych. Rzeczywisty rozkład takiego obciążenia jest sprzeczny z modelem przedstawionym w normie EN 1993-1-1. W artykule przeprowadzono analizę numeryczną wpływu kształtu dźwigara kratowego z imperfekcjami geometrycznymi na obciążenie poprzecznego tężnika połaciowego. Uwzględniono stosowane najczęściej kształty dźwigarów oraz wybrane parametry geometryczne. Uzyskane wyniki wykorzystano do określenia obciążenia działającego na płatwie oraz pręty stężeń typowej konstrukcji hali.

**Słowa kluczowe:** geometria kratownicy, stężenie, imperfekcje geometryczne

# 1. Introduction

In order to design hall structures in which steel trusses act as truss girders, the proper design of transverse and longitudinal roof bracings is crucial. Transverse roof bracings play a vital role as they stabilise the upper chords of trusses against out-of-plane buckling by reducing the chords' buckling lengths. In the case of roofs without purlins, bracing can be replaced by structural trapezium-shaped sheets from roof envelopes. Both the transverse roof bracing and the trapezium-shaped sheet can transmit environmental loads such as wind pressure on front walls or technological loads, for example, forces caused by the acceleration or deceleration of cranes. For this reason, both the transverse roof bracing and the trapezium-shaped sheet should have appropriate levels of stiffness in order to prove effective in the structure [1, 5]. While designing these elements, loads generated by the truss girder resulting from geometrical imperfections of the truss girder should also be taken into consideration. This imperfection, in the form of curvature of the compressed chord, generates a horizontal load which can be represented as nodal loads in the case of roof bracing and, in the case of the trapezium-shaped sheet, as a distributed load.

The load of roof bracing resulting from the imperfection of the truss girder's compression chord can be determined using the guidelines set in accordance with the EN 1993-1-1 standard which assumes a parabolic shape of the imperfection. This load is related both to the maximum compression force of chord  $N_{Ed}$  and the value of imperfection  $e_0$  equal to  $L/500$  ( $L$  – length of the compression chord). The number of braced girders  $m$  is taken into account by coefficient  $\alpha_m$  and the stiffness of the roof bracing is taken into account by additional deformation  $\delta_d$  which is calculated iteratively. The load of roof bracing thus determined is uniformly distributed because the equations indicated in the standard [7] are based on the analogy of horizontal thrust in a parabolic arch under a uniformly distributed load. In addition, this load should be self-balanced and should consider elastic deformation of the roof bracing  $\delta_d$  resulting from load  $q$  and other loads (e.g. wind pressure on front wall) which are presented in Fig. 1.

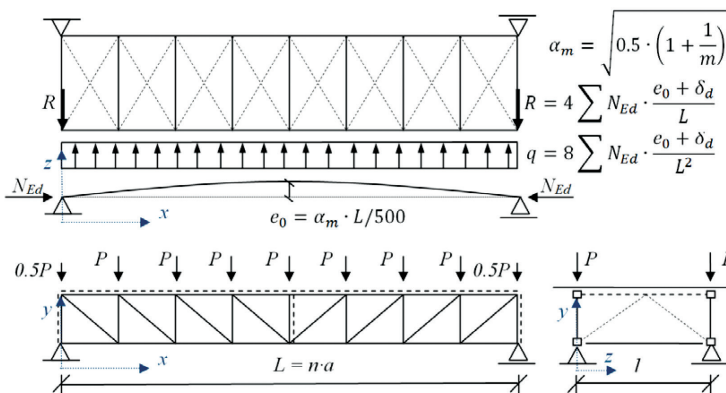


Fig. 1. Standard-indicated notional load of transverse roof bracing originating from a girder with imperfections

Recent theoretical analyses [3, 6] and experimental research [8] reveal that the standard modelling of the bracing load resulting from the imperfection of truss girders does not

correspond to reality due to numerous simplifications of the standard model, which are described in detail in previous papers [3, 6]. The author's theoretical models, which are recommended in the papers, demonstrate that the actual load of roof bracing  $q(x)$  is non-uniform and sign-changing within the distance of around  $L/4$  from the supports in the case of a single-span truss. Additionally, it has been proven that the values of nodal load generated by the trusses on roof bracing may be much higher than the values of the analysis performed in accordance with EC3 (Fig. 2). The recommended models make it possible to calculate the value of the nodal load on roof bracing in a simple way while considering the following factors:

- ▶ various deformations of compressed chord, e.g. sinusoidal, parabolic or complex;
- ▶ any distributions of longitudinal force in the chord;
- ▶ simultaneous initial imperfection of the bottom chord;
- ▶ sway imperfection of the whole truss.

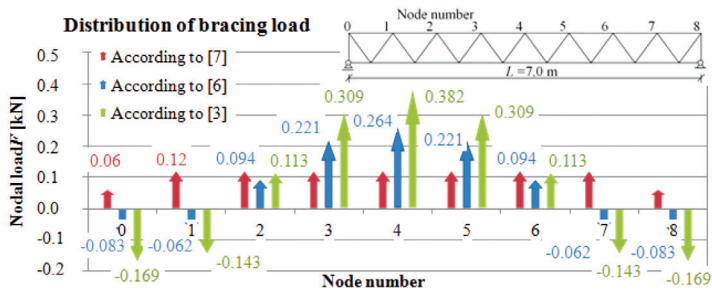


Fig. 2. Standard and theoretical load of bracing

The experimental research which is presented in paper [8] confirmed the non-uniform and sign-changing distribution of the bracing load resulting from the imperfection of truss. Tests on seven meter long models of truss with parallel chords and V-type web members are described in the paper. As an out-of-plane imperfection, the sinusoidal shape of a compressed chord was adopted. In the experimental research, the imperfection value of  $e_0 = L/175 = 40$  mm was adopted. An example of nodal load distribution of roof bracing resulting from research model [8] and calculated according to the empirical guidelines [6] is presented in Fig. 2.

At the testing stage, horizontal reactions of transverse supports fixed to selected nodes of chords were measured. The obtained results were confirmed by the relevant numerical analysis (Fig. 3).

Certain quantitative differences between empirical (Fig. 2) and experimental (Fig. 3) values result from the elastic deformation of the bottom chord, which has been indicated in paper [4].

Commonly used in hall structures, truss girders are characterised by diverse geometry depending on the intended use of the hall structure, the type of roof cladding system or architectural factors. These geometries can evidently have a quantitative influence on the distribution of the roof bracing load as the imperfection value  $e_0$  is based on the length of chord  $L$ . In the case of a truss with arched and pitched chords, this length depends on the inclination of the roof and the arch height. Therefore, it may be different in the case of trusses

with the same support spacing but with different geometry. An additional factor possibly influencing the nodal load of an imperfect truss on roof bracing is truss height due to the influence of the inclination of webs; this was proven in papers [3] and [6].

The indicated relationships were derived empirically and confirmed experimentally only in the case of a truss with parallel chords. It is therefore justified to conduct relevant numerical parametric analyses which consider different geometries of truss girders applied in practice.

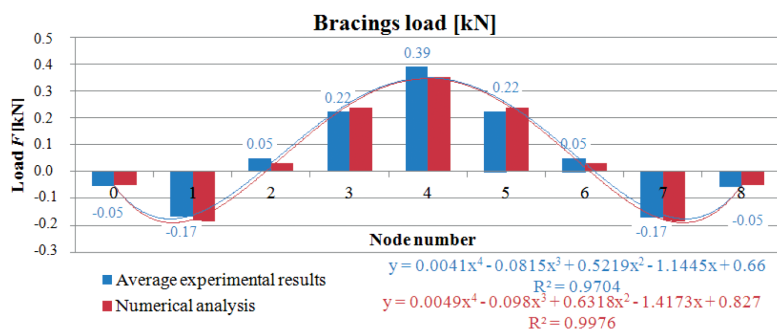


Fig. 3. Experimental results [6]

## 2. Numerical model and analysis

Parametric analyses were conducted using single-span steel trusses with a length between supports of  $L = 24.0$  m (not in the case of truss purlin – G10\*). The numerical analysis of the influence of the static scheme is presented in paper [2]. In this analysis, three variable parameters were considered:

- ▶ geometric shape of truss;
- ▶ height of the truss with parallel chords;
- ▶ inclination of roof or height of arch (in the case of arched truss girders).

An example of truss geometry and the numbering of the upper chord nodes are presented in Fig. 4.

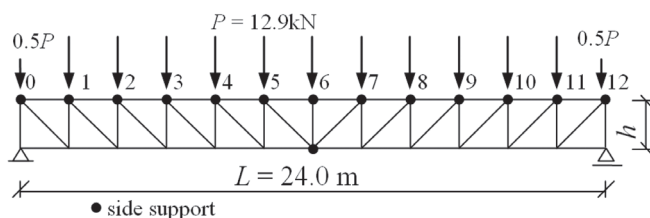


Fig. 4. Dimensions of the truss and numbering of the nodes of the upper chord

Only the gravitational load of  $P = 12.9$  kN, which was applied to the nodes of the upper chord, and typical N-type web members were considered in the parametric analysis. This load, as well as the geometry shown in Fig. 4, were used to determine the probable cross sections of particular truss elements. Having completed a static analysis and design procedure in accordance with [7], chords with a HEB 140 cross section and web members with a SH 100 x 6 cross section were adopted.

The examined truss girders are presented in Fig. 5. The value of  $h = 2.0$  m was adopted as the basic truss height. In the case of trusses with a lowered bottom chord, axial height from the lowered chord to the fulcrum was adopted as height  $h$ . This height was graded for G1-G7 geometries every 0.5 m from the basic value  $h = 2.0$  m to the value  $h = 4.0$  m. With regard to pitched trusses, G2-G5 and G8 geometries, the inclination angles of upper chords from  $3^\circ$  to  $15^\circ$  were considered. In the case of arched truss girders, G6, G7 and G9 geometries, heights of arched chord from  $f = 0$  to  $f = L/7.5$  were considered.

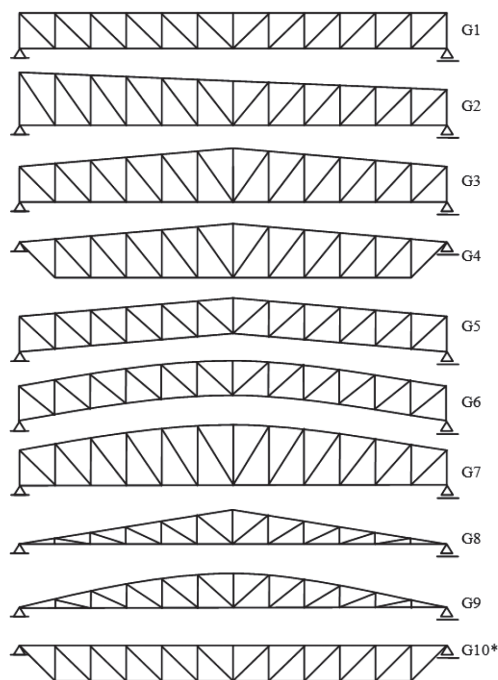


Fig. 5. Geometry of examined truss girders

In each case, transverse roof bracing was modelled as a rigid support system due to displacement in the direction transverse to the plane of truss. These supports were located in each node of the upper chord and in the mid-span of the bottom chord (Fig. 4).

In the case of G1-G7 geometries, the value  $h = 2.0$  m was used as the basic height of truss. In the case of G2-G5 and G8 geometries, the value of  $3^\circ$  was used as the basic inclination of the upper chord. For G6, G7 and G9 geometries, the value  $f = L/40$  was used as the basic arch height of the upper chord.

G10\* geometry corresponds to the typical structural solutions of truss purlins. In typical structures, truss purlins attain a span length of around 12.0–18.0 m. For the purposes of parametric analysis in the case of G10\* geometry, the length  $L = 12.0$  m, the height  $h = 0.5$  m and the gravitational load  $P = 2.15$  kN were adopted.

Parametric analyses were conducted by means of the SOFiSTiK program [9] using its text module for parametric description of the analysed trusses. A geometrically and materially

non-linear analysis with geometric imperfections was performed. A bi-linear elasto-plastic model of material with parameters corresponding to S235 steel was considered. The analysed trusses were modelled using beam-type finite elements with six degrees of freedom at each node. The distance between the truss joints was divided into twenty finite elements. A sinusoidal shape of imperfection in the upper chord was adopted. Its value  $e_0$  was  $L/500$  ( $L$  – length of compressed chord). Geometric imperfection was modelled directly by changing the coordinates of all finite element nodes of the upper chord. Rigid connections between webs and chords were adopted.

In each analysed case, the nodal load of the bracing was calculated as specified by standard [7]. These values are given in square brackets in Figs. 6, 7, 8 and 9.

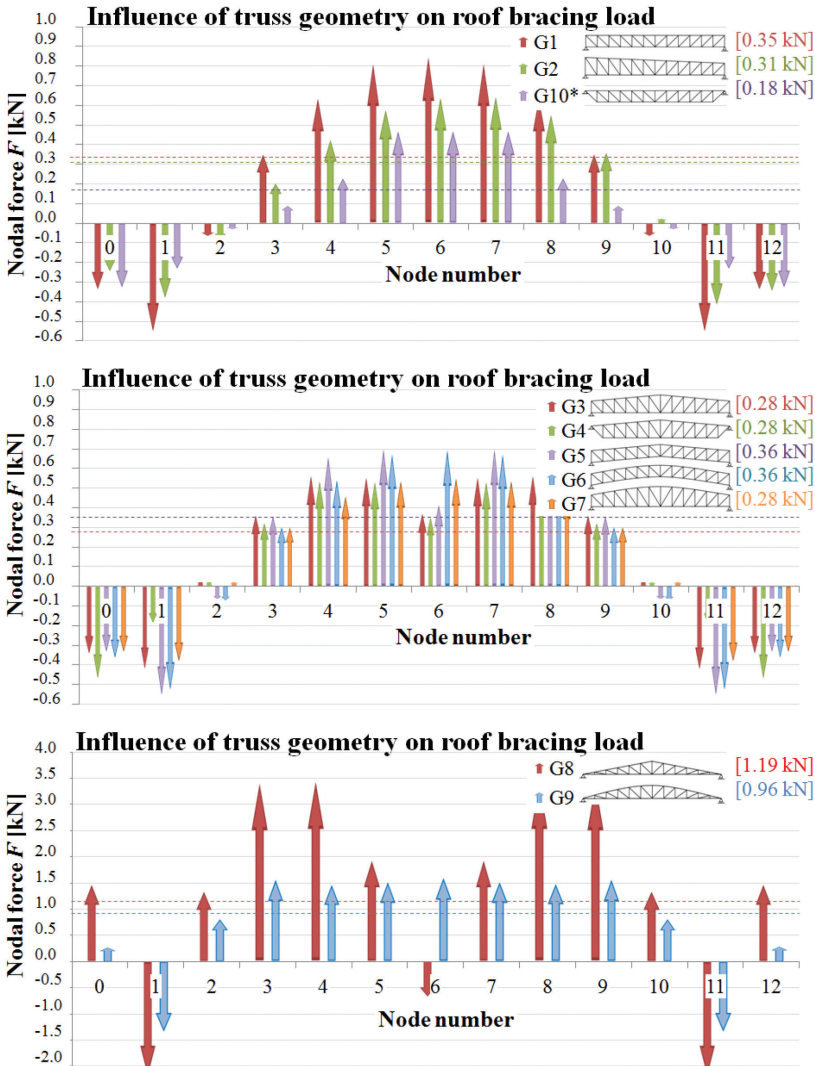


Fig. 6. Influence of truss geometry on roof bracing load

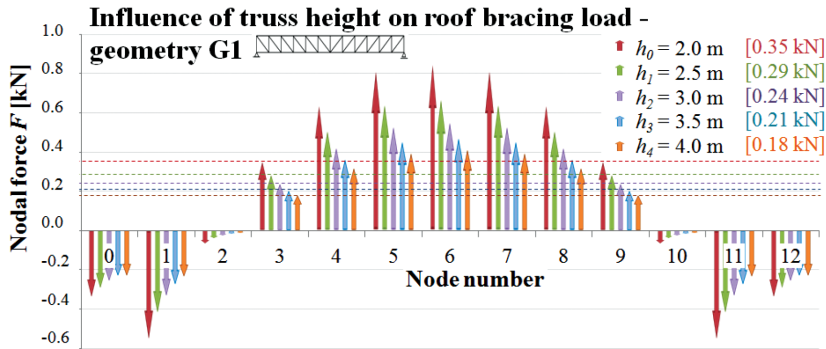


Fig. 7. Influence of truss height on roof bracing load

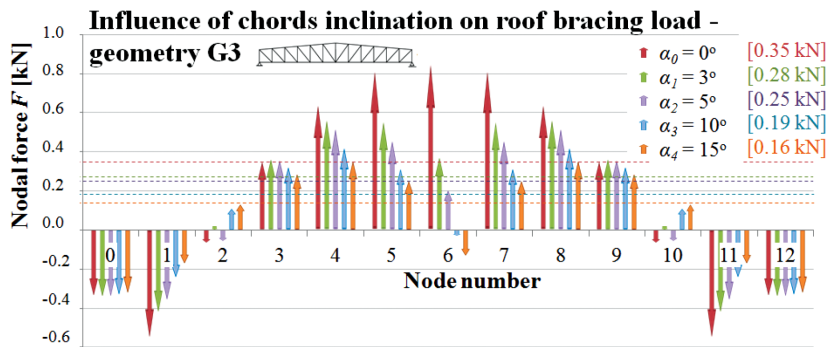


Fig. 8. Influence of chords inclination on roof bracing load

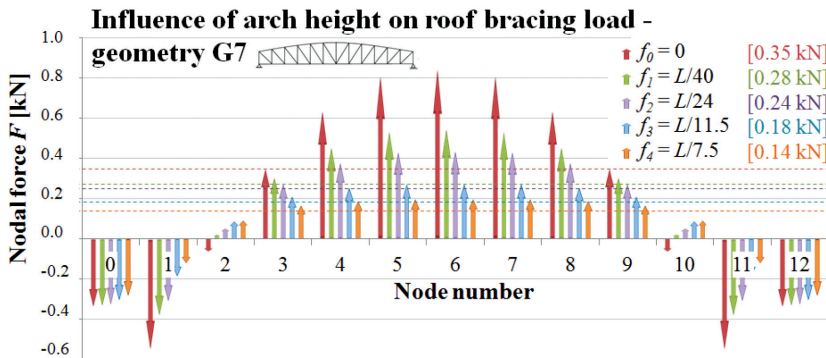


Fig. 9. Influence of arch height on roof bracing load

### 3. Results

The results of the numerical analyses are presented in Tables 1–4, in which the load of roof bracing  $F_n$  [kN] is included. Considering the symmetry of loads in most results, only the results for nodes 0-6 are provided. Selected results were translated to graph form in order to determine the influence of particular parameters. Table 1 presents the load of roof bracing

in the case of different geometries of truss girders and with the basic values of truss/arch height as well as roof inclination. The positive load values shown in the tables and graphs are complies with standard load sign.

Table 1. Test results – Influence of geometry ( $h = 2.0$  m,  $\alpha = 3^\circ$ ;  $f = L/40$ ) [kN]

Geometry	Node number						
	0	1	2	3	4	5	6
G1	-0.34	-0.55	-0.07	0.35	0.64	0.81	0.85
G2	-0.24	-0.38	-0.08	0.20	0.43	0.58	0.64
G3	-0.34	-0.42	0.02	0.36	0.57	0.56	0.37
G4	-0.47	-0.18	0.02	0.33	0.54	0.54	0.35
G5	-0.34	-0.56	-0.07	0.36	0.66	0.70	0.41
G6	-0.36	-0.53	-0.07	0.30	0.54	0.67	0.70
G7	-0.34	-0.39	0.02	0.30	0.46	0.54	0.55
G8	1.47	-2.18	1.34	3.41	3.44	1.93	-0.67
G9	0.28	-1.34	0.81	1.57	1.58	1.53	1.61
G10*	-0.33	-0.23	-0.03	0.09	0.26	0.47	0.47

The findings concerning the influence of truss height on the load of roof bracing are presented in Table 2. The analysis was conducted in the case of G1 geometry and the following truss heights were considered:  $h_0 = 2.0$  m;  $h_1 = 2.5$  m;  $h_2 = 3.0$  m;  $h_3 = 3.5$  m;  $h_4 = 4.0$  m.

Table 2. Analysis results – Influence of truss height [kN]

Height	Node number						
	0	1	2	3	4	5	6
$h_0$	-0.34	-0.55	-0.07	0.35	0.64	0.81	0.85
$h_1$	-0.29	-0.42	-0.04	0.28	0.51	0.64	0.67
$h_2$	-0.26	-0.34	-0.03	0.24	0.41	0.53	0.55
$h_3$	-0.23	-0.28	-0.02	0.21	0.36	0.45	0.47
$h_4$	-0.21	-0.24	-0.01	0.18	0.32	0.41	0.41

Analysis results regarding the influence of the inclination of the truss chord on the load of roof bracing are presented in Table 3. In this case, G3 geometry was adopted as the basic geometry. The following inclination angles were considered in the analysis:  $\alpha_0 = 0^\circ$ ;  $\alpha_1 = 3^\circ$ ;  $\alpha_2 = 5^\circ$ ;  $\alpha_3 = 10^\circ$ ;  $\alpha_4 = 15^\circ$ .



Table 3. Analysis results – Influence of chords inclination [kN]

Inclination	Node number						
	0	1	2	3	4	5	6
$\alpha_0$	-0.34	-0.55	-0.07	0.35	0.64	0.81	0.85
$\alpha_1$	-0.34	-0.42	0.02	0.36	0.57	0.56	0.37
$\alpha_2$	-0.34	-0.36	0.06	0.36	0.52	0.46	0.20
$\alpha_3$	-0.33	-0.24	0.11	0.32	0.42	0.32	-0.03
$\alpha_4$	-0.32	-0.17	0.13	0.29	0.35	0.25	-0.13

The analysis results regarding the influence of arch height of truss on the load of roof bracing are presented in Table 4. In this case, G7 geometry was adopted as the basic geometry. The following arch heights:  $f_0 = 0$ ;  $f_1 = L/40$ ;  $f_2 = L/24$ ;  $f_3 = L/11.5$ ;  $f_4 = L/7.5$  were considered in the analysis.

Table 4. Analysis results – Influence of arch height [kN]

Arch height	Node number						
	0	1	2	3	4	5	6
$f_0$	-0.34	-0.55	-0.07	0.35	0.64	0.81	0.85
$f_1$	-0.34	-0.39	0.02	0.30	0.46	0.54	0.55
$f_2$	-0.33	-0.31	0.05	0.27	0.38	0.43	0.44
$f_3$	-0.31	-0.19	0.09	0.21	0.26	0.27	0.27
$f_4$	-0.28	-0.12	0.09	0.17	0.19	0.20	0.20

The results presented in Tables 1–4 are displayed in graph form in Figs. 6–10.

The results regarding the influence of truss girder geometries on the load of roof bracing (Fig. 6) are in good agreement with the results of theoretical analyses [3, 6] and experimental research [8]. In all cases, non-uniform distribution of bracing's load with the sign-changing points near the supports was occurred. In all studies, the maximum values of nodal load are higher than the values specified by standards.

It should be pointed out that in the case of the G3, G4, G5 geometries, a noticeable reduction of nodal load in the middle of the span was observed. This is connected with the ridge of the upper chord. In the case of the G6 and G7 geometries, the alignment of load distribution occurs in the middle of span.

The cases of G8 and G9 geometries, which are presented in Fig. 6, show significant changes in the distribution of the load of roof bracing. In the case of the G8 geometry, an additional sign changing of the nodal load in the ridge was observed. However, in the case of the G9



geometry, a quasi-uniformly distributed load (approximately 150% of the value of standard load) occurred across the whole mid-span of truss.

According to the paper [6], inclination of the truss which results from the curvature of the upper chord has a major influence on the bracing's load. The resulting twisting angle of the truss cross section depends on truss height. The influence of the height of the truss with the G1 geometry on the load of roof bracing (Fig. 7) is characterised by a non-uniform reduction in each node. The biggest reduction occurs in trusses of insignificant height. However, in the case of trusses higher than 3.0 m, this influence is negligible.

In the case of trusses with non-parallel chords, the distribution of compression force in the upper chord is different than the quasi-parabolic distribution. It was reflected in the distribution of the load of roof bracing (Fig. 8) by reducing the value of nodal load in the ridge area. Regarding the analysed trusses with the chord inclination angle above  $10^\circ$ , additional sign changing of load occurred in the ridge node.

The most significant influence of the upper chord arch height on the nodal load of the roof bracing was observed in the mid-span zone of truss. An increase in arch height was accompanied by alignment of nodal load in this zone. In the analysed truss with an arch height of  $f_4 = L/7.5$ , the value of nodal load in all the nodes from 3 to 9 was approximately 140% of the value of standard load.

#### 4. Roof bracing

The above-determined the load of roof bracing resulting from truss girder imperfection was applied to the transverse roof bracing of the hall structure shown in Fig. 10. Ten truss frames ( $m = 10/2$ ) with the spacing  $l = 6.0$  m and two X-type bracings located in the first and last sections of the hall were adopted. As recommended by the standard [7], the relevant value of reduction

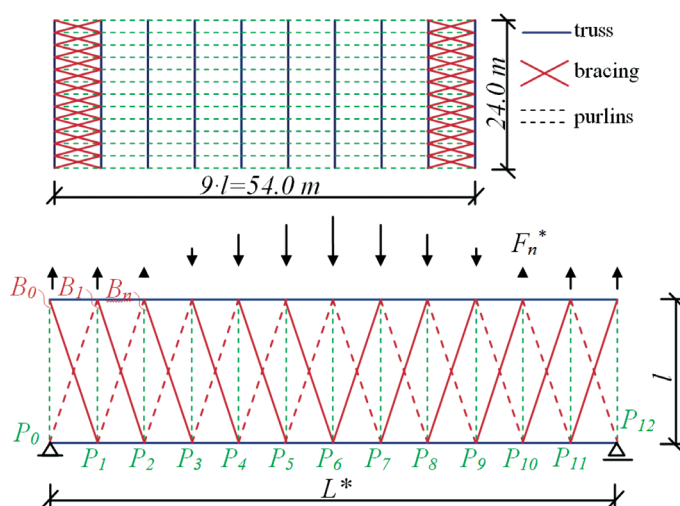


Fig. 10. Adopted hall structure and bracing geometry

coefficient  $\alpha_m$  was used. The bracing length  $L^*$  was calculated as the length of the upper chord in the relevant cases of geometry. Circular rods with a diameter of  $\phi = 20$  mm as bracing rods and a IPE 180 I-section rods as purlins were adopted. The value of nodal load applied to the bracing  $F_n^*$  was calculated in accordance with the procedure set in the EN 1993-1-1 standard ( $F_n^* = F_n \cdot \alpha_m \cdot m$ ).

Both sign-changing distribution of the of the roof bracing and higher values of nodal load have an impact on the load of particular elements of bracing and purlins. The relevant values of the forces in bracing rods and purlins for selected cases of geometry were determined by means of numerical analysis performed on a model built of beam-type elements. The analyses were conducted using the SOFiSTiK program [9] by applying a geometrically non-linear analysis of the bracing model presented in Fig. 12. Bracing rods were modelled as cable elements. The results regarding the load of particular elements of the bracing model are presented in Tables 5 and 6.

Table 5. Numerical analysis of separated roof bracings – load of purlins

Geometry	Purlin number						
	0	1	2	3	4	5	6
G1 ( $h_0$ )	4.86 (7.99)	6.09 (7.29)	8.12 (6.01)	8.42 (4.67)	7.12 (3.34)	4.69 (2.00)	3.22 (1.33)
G1 ( $h_4$ )	2.51 (4.11)	3.28 (3.75)	4.17 (3.09)	4.22 (2.40)	3.55 (1.72)	2.34 (1.03)	1.56 (0.68)
G2	3.22 (7.08)	4.09 (6.45)	5.50 (5.32)	5.82 (4.13)	5.08 (2.96)	3.44 (1.77)	2.42 (1.18)
G3 ( $\alpha_1$ )	3.59 (6.39)	4.83 (5.83)	6.39 (4.80)	6.34 (3.73)	5.00 (2.67)	2.86 (1.60)	1.48 (1.06)
G3 ( $\alpha_4$ )	1.78 (3.65)	2.98 (3.33)	3.60 (2.75)	3.13 (2.13)	2.04 (1.53)	0.91 (0.91)	-0.09 (0.61)
G4	3.65 (6.39)	5.40 (5.83)	6.07 (4.50)	6.00 (3.73)	4.77 (2.67)	2.074 (1.60)	1.37 (1.06)
G5	3.68 (8.22)	4.91 (7.50)	6.98 (6.18)	7.28 (4.80)	5.94 (3.43)	3.47 (2.06)	1.62 (1.36)
G6	3.47 (8.22)	4.78 (7.50)	6.74 (6.18)	7.04 (4.80)	5.92 (3.43)	3.87 (2.06)	2.65 (1.36)
G7 ( $f_1$ )	3.32 (6.39)	4.56 (5.83)	6.01 (4.80)	5.97 (3.73)	4.84 (2.67)	3.10 (1.60)	2.09 (1.06)
G7 ( $f_4$ )	1.34 (3.20)	2.38 (2.91)	2.83 (2.40)	2.51 (1.87)	1.87 (1.33)	1.14 (0.80)	0.76 (0.53)
G8	34.84 (27.2)	28.77 (24.8)	36.78 (20.4)	32.09 (15.9)	19.32 (11.4)	7.13 (6.8)	-0.59 (4.5)
G9	20.09 (21.9)	18.84 (20.0)	23.71 (16.5)	20.87 (12.8)	14.94 (9.2)	8,90 (5,5)	6,09 (3,6)
G10*	1.75 (3.99)	2.88 (3.57)	3.68 (0.62)	3.81 (2.99)	3.47 (2.33)	2.55 (1.00)	1.74 (0.66)



Table 6. Numerical analysis of separated roof bracings – load of bracing rods

Geometry	rod number					
	0	1	2	3	4	5
G1 ( $h_0$ )	-6.50 (-7.61)	-8.56 (-6.33)	-8.86 (-4.91)	-7.47 (-3.51)	-4.94 (-2.11)	-1.66 (-0.69)
G1 ( $h_4$ )	-3.49 (-3.91)	-4.39 (-3.26)	-4.45 (-2.52)	-3.73 (-1.80)	-2.46 (-1.08)	-0.81 (-0.35)
G2	-4.37 (-6.74)	-5.80 (-5.61)	-6.13 (-4.35)	-5.33 (-3.11)	-3.63 (-1.87)	-1.28 (-0.61)
G3 ( $\alpha_1$ )	-5.16 (-6.09)	-6.72 (-5.07)	-6.67 (-3.93)	-5.24 (-2.81)	-2.99 (-1.69)	-0.76 (-0.55)
G3 ( $\alpha_4$ )	-3.17 (-3.48)	-3.78 (-2.90)	-3.29 (-2.24)	-2.14 (-1.60)	-0.74 (-0.96)	-0.17 (-0.31)
G4	-5.72 (-6.09)	-6.41 (-5.07)	-6.31 (-3.93)	-5.00 (-2.81)	-2.87 (-1.69)	-0.72 (-0.55)
G5	-5.26 (-7.83)	-7.35 (-6.52)	-7.66 (-5.05)	-6.23 (-3.61)	-3.62 (-2.17)	-0.86 (-0.71)
G6	-5.12 (-7.83)	-7.10 (-6.52)	-7.41 (-5.05)	-6.22 (-3.61)	-4.08 (-2.17)	-1.37 (-0.71)
G7 ( $f_1$ )	-4.88 (-6.09)	-6.32 (-5.07)	-6.28 (-3.93)	-5.09 (-2.81)	-3.26 (-1.69)	-1.08 (-0.55)
G7 ( $f_4$ )	-2.54 (-3.04)	-2.97 (-2.53)	-2.64 (-1.96)	-1.96 (-1.40)	-1.20 (-0.84)	-0.39 (-0.27)
G8	-30.72 (-25.9)	-38.69 (-21.5)	-33.58 (-16.7)	-20.19 (-11.9)	-6.51 (-7.2)	-0.70 (-2.3)
G9	-20.01 (-20.9)	-24.88 (-17.4)	-21.91 (-13.5)	-15.70 (-9.6)	-9.39 (-5.8)	-3.14 (-1.9)
G10*	-3.15 (-3.65)	-3.86 (-3.14)	-4.02 (-2.44)	-3.65 (-1.74)	-2.62 (-1.05)	-0.86 (-0.33)

In each case, the load of a particular member, which was determined on the basis of the standard value of the bracing's load, is given in brackets. In both Tables 5 and 6, longitudinal compression force is indicated by a '+' sign.

## 5. Conclusions

Nodal load distributions of transverse roof bracing resulting from the geometrical imperfection of truss girders (presented in Figs. 6–11) show strong agreement with the theoretical and experimental analyses. The analysed truss geometries have a negligible influence on the nodal load distribution of roof bracing. In most cases, load distribution approximates the load distribution obtained in the truss with parallel chords (G1). Only

in the case of the triangular truss (G8) can a change in load distribution characterised by multiple sign changing be observed.

An increase in truss height (in the case of the G1 geometry) reduces the value of the nodal load, which results from the evident reduction of compression force in the upper chord and the reduction of the twisting angle of the truss cross section. This angle depends on shape of chord imperfection. Therefore, this influence is the highest in the central part of the truss.

Considerable influence of the chord ridge (G3, G4, G5) and curvature (G6, G7) has been observed. The influence of the compressed chord's ridge manifests itself in the reduction of nodal load on the roof bracing in the ridge area. An increase in chord inclination (above  $10^\circ$ ) considerably influences the reduction of load, which may lead to its sign changing. The influence of the curvature of the compressed chord manifests itself by alignment of the load values in the central part of truss. Increasing the upper chord arch height to the value of  $f = L/7.5$  leads to the alignment of nodal load values in the entire central part of the truss (ranging from  $0.25L$  to  $0.75L$ ).

Load distribution of transverse roof bracing influences the distribution of longitudinal force in purlins and bracing rods. In the case of bracing load distribution specified by the standard (uniform distribution), eaves purlins (P0) and bracing rods in extreme fields (B0) are the most loaded. The non-uniform distribution of load obtained in the analysed cases increases the load of purlins and bracing rods in the area of load sign changing (purlins P2, P3 and bracing rods B1, B2).

In the case of non-uniform distribution, the maximum compression forces in purlins resulting from numerical analysis are 8.42 kN in the case of the G1 geometry and 36.78 kN in the case of the G8 geometry. These forces are similar to the maximum load of purlins in the case of the standard load. They constitute 16 and 70% respectively of the out-of-plane buckling resistance for compression of the analysed purlin.

The maximum values of tensile force in bracing rods are 8.86 kN in the case of the G1 geometry and 38.69 kN in the case of G8 geometry. These values, which are higher than the values of the forces obtained in the case of standard load (in the case of the G1 geometry, up to 16%, and in the case of the G8 geometry, up to 50%). They constitute 12 and 52% respectively of the bracing rod's tension resistance. It should therefore be recognised that they contribute to ensuring safety of the designed element.

None of the obtained load distributions approximate the distribution indicated by the EN 1993-1-1 standard. It can therefore be concluded that, in the case of currently designed trusses with diverse geometries, standard recommendations are confusing for designers and lead to the erroneous estimation of load for particular purlins and bracing rods. This explains why EN 1993-1-1 regulations should be verified. This can be achieved by changing the shape and the value of the bracing standard load distribution or by replacing the simplified flat model with the spatial model. This model should include a separated fragment of a hall (most often two main frames) and its existing roof bracings, vertical truss girder bracings and wall bracings.



## References

- [1] Biegus A., *Trapezoidal sheet as a bracing preventing from out-of-plane buckling*, Archives of Civil and Mechanical Engineering 15/2015, 735–741.
- [2] Biegus A., Czepizak D., *Analytical and numerical research of equivalent stabilizing force of stiffened truss chords*, Matec Web of Conferences 262/2019.
- [3] Czepizak D., Biegus A., *Refined calculation of lateral bracing systems due to global geometrical imperfection*, Journal of Constructional Steel Research 19/2016, 30–38.
- [4] Niewiadomski L., Zamorowski J., *The load of transversal bracings resulting from geometric imperfection of single-span trusses of roofs*, Proceedings of the 12<sup>th</sup> International Conference on New Trend in Static and Dynamics of Buildings, Bratislava, Slovakia, 2014. [in Polish]
- [5] Pałkowski S., *The calculation models of transversal roof bracings*, Inżynieria i Budownictwo 3/2016, 131–133.
- [6] Pałkowski Sz., Piątkowski M., *On the calculation of lateral roof bracing*, Inżynieria i Budownictwo 4/2014, 210–213.
- [7] PN-EN 1993-1-1: 2006. Eurocode 3: Design of steel structures. Part 1-1: General rules and rules for building.
- [8] Piątkowski M., *Impact of truss girder geometrical imperfections on roof bracing load*, Matec Web of Conferences 262/2019.
- [9] SSD SOFiSTiK Structural Desktop, User interface of SOFiSTiK, SOFiSTiK AG, 2008.